motion of crystalline domains in an otherwise rigid solid-state system. □

Received 7 January; accepted 10 June 2002; doi:10.1038/nature00901.

1. Huang, S. Y., Kavan, L., Exnar, I. & Grätzel, M. J. Rocking chair lithium battery based on nanocrystalline TiO_2 (anatase). *J. Electrochem. Soc.* **142,** L142–L144 (1995).
2. Ohzuku, T., Kodama, T. & Hirai, T. Electrochemistry of anatase titanium dioxide in lithium non-aqueous cells. *J. Power Sources* **14,** 153–166 (1985).
3. Ohzuku, T. & Hirai, T. An electrochromic display based on titanium dioxide. *Electrochim. Acta* **27,** 1263–1266 (1982).
4. Ottaviani, M., Panero, S., Morzilli, S. & Scrosati, B. The electrochromic characteristics of titanium oxide thin film electrodes. *Solid State Ionics* **20,** 197–202 (1986).
5. Cantao, M. P., Cisneros, J. I. & Torresi, R. M. Electrochromic behaviour of sputtered titanium-oxide thin-films. *Thin Solid Films* **259,** 70–74 (1995).
6. Bechinger, C., Ferrere, S., Zaban, A., Sprague, J. & Gregg, B. A. Photoelectrochromic windows and displays. *Nature* **383,** 608–610 (1996).
7. O'Regan, B. & Grätzel, M. A low-cost, high-efficiency solar-cell based on dye-sensitised colloidal TiO_2 films. *Nature* **353,** 737–740 (1991).
8. Hagfeldt, A. & Grätzel, M. Light-induced redox reactions in nanocrystalline systems. *Chem. Rev.* **95,** 49–68 (1995).
9. Wagemaker, M., van de Krol, R., Kentgens, A. P. M., van Well, A. A. & Mulder, F. M. Two phase morphology limits lithium diffusion in TiO_2 (anatase): A Li-7 MAS NMR study. *J. Am. Chem. Soc.* **46,** 11454–11461 (2001).
10. Xu, Z. & Stebbins, J. F. Cation dynamics and diffusion in lithium orthosilicate — 2-dimensional Li-6 NMR. *Science* **270,** 1332–1334 (1995).
11. Verhoeven, V. W. J. *et al.* Lithium dynamics in $LiMn_2O_4$ probed directly by two-dimensional Li-7 NMR. *Phys. Rev. Lett.* **86,** 4314–4317 (2001).
12. Ernst, R. R., Bodenhausen, G. & Wokaun, A. *Principles of Nuclear Magnetic Resonance in One and Two Dimensions* (Clarendon, Oxford, 1994).
13. Lunell, S., Stashans, A., Ojamae, L., Lindstrom, H. & Hagfeldt, A. Li and Na diffusion in TiO_2 from quantum chemical theory versus electrochemical experiment. *J. Am. Chem. Soc.* **119,** 7374–7380 (1997).
14. Kavan, L., Grätzel, M., Gilbert, S. E., Klemenz, C. & Schell, H. J. Electrochemical and photoelectrochemical investigation of single-crystal anatase. *J. Am. Chem. Soc.* **118,** 6716–6723 (1996).
15. Claus, J., Schmidt-Rohr, K. & Spiess, H. W. Determination of domain sizes in heterogeneous polymers by solid-state NMR. *Acta Polym.* **44,** 1–17 (1993).
16. Schmidt-Rohr, K. & Spiess, H. W. *Multidimensional Solid-state NMR and Polymers* (Academic, London, 1994).
17. Koudriachova, M. V., Harrison, N. M. & de Leeuw, S. W. Effect of diffusion on lithium intercalation in titanium dioxide. *Phys. Rev. Lett.* **86,** 1275–1278 (2001).

Acknowledgements

This work is a contribution from the Delft Institute for Sustainable Energy (DISE).

Competing interests statement

The authors declare that they have no competing financial interests.

Correspondence and requests for materials should be addressed to F.M.M. (e-mail: mulder@iri.tudelft.nl).

Synthetic hosts by monomolecular imprinting inside dendrimers

Steven C. Zimmerman*†, Michael S. Wendland*, Neal A. Rakow*, Ilya Zharov† & Kenneth S. Suslick*†

** Department of Chemistry; † Beckman Institute for Advanced Science and Technology, University of Illinois at Urbana-Champaign, 600 S. Mathews Avenue, Urbana, Illinois 61801, USA*

Synthetic host systems capable of selectively binding guest molecules are of interest for applications ranging from separations and chemical or biological sensing to the development of biomedical materials. Such host systems can be efficiently prepared by 'imprinting' polymers or inorganic materials with template molecules, which, upon removal, leave behind spatially arranged functional groups that act as recognition sites[1–4]. However, molecularly imprinted polymers have limitations, including incomplete template removal, broad guest affinities and selectivities, and slow mass transfer[5–8]. An alternative strategy for moulding desired recognition sites uses combinatorial libraries of assemblies that are made of a relatively small number of molecules, interconverting in dynamic equilibrium; upon addition of a target molecule, the library equilibrium shifts towards the best hosts[9–11]. Here we describe the dynamic imprinting of dendritic macromolecules with porphyrin templates to yield synthetic host molecules containing one binding site each. The process is based on our general strategy to prepare cored dendrimers[12,13], and involves covalent attachment of dendrons to a porphyrin core, cross-linking of the end-groups of the dendrons, and removal of the porphyrin template by hydrolysis. In contrast to more traditional polymer imprinting, our approach ensures nearly homogeneous binding sites and quantitative template removal. Moreover, the hosts are soluble in common organic solvents and amenable to the incorporation of other functional groups, which should facilitate further development of this system for novel applications.

When developing our 'monomolecular imprinting' methodology, we selected dendrimers as macromolecular hosts because their molecular homogeneity and excellent solubility facilitate characterization[14]. The choice of a porphyrin as templating agent was motivated by the scarce availability of synthetic hosts for large molecule guests[15] and the fact that porphyrins are excellent probes of binding, owing to the sensitivity of their intense colour to the local environment[16]. Porphyrins have been integrated into molecularly imprinted polymers[17] and synthetic hosts[18], but have to our knowledge not been used as templates. Moreover, the chemistry of porphyrin-core dendrimers is well established, given their role as well-studied synthetic models of haem proteins and related proteins[19–22].

The basic strategy for synthesizing dendrimer hosts follows our earlier work on cored dendrimers[12,13]. The preparation of porphyrin-core dendrimer **1** is summarized in Fig. 1. The key structural features of this pre-cross-linked dendrimer are the tetrakis-meso(3,5-dihydroxyphenyl)-porphyrin (**3**)[19] unit at the core, and hydrolysable ester-bond links to eight third-generation Fréchet-type dendrons[23] (**2**)[12], which give a total of 64 homoallyl end-groups (see Supplementary Information). In addition to **1**, a small amount (~5%) of dendrimers containing six or seven dendrons was formed (see below).

Porphyrin-core dendrimer **1** was cross-linked[12] using 4 mol% (per alkene) of Grubbs' catalyst **4**[24] at 10^{-6} M in benzene to produce cross-linked dendrimer **5** in 88% yield. Size exclusion chromatography (SEC) established that cross-linking occurs largely (≥95%) intramolecularly. The ^{1}H NMR spectrum of **5** confirmed the formation of internal, disubstituted alkene groups and gave the average number of cross-links as approximately 29. The matrix-assisted laser desorption/ionization–time of flight (MALDI–TOF) mass spectrum of **5** provided conclusive evidence for extensive intramolecular cross-linking: it contained peaks corresponding to individual isomers from 28 to 32 out of 32 possible cross-links (mass/charge ratios (m/z) 10,369, 10,341, 10,313, 10,285, 10,257), with the tallest peak at m/z 10,285 (31 cross-links, see Supplementary Information). The ability of catalyst **4** to produce from **1** a compact structure with a median of 30 out of 32 possible cross-links may be due to the reversibility of the ring closing metathesis (RCM) reaction[24]. The precise details of the cross-linking process remain to be determined. But analogy with the quantitative RCM of polyolefins[25] suggests that it may be a dynamic process, thus ensuring that millions of kinetically favoured cross-link isomers may equilibrate into a small number of thermodynamically stable ones.

Treatment of the cross-linked dendrimer **5** with 2.5 M aqueous KOH solution in tetrahydrofuran (THF) quantitatively removed the porphyrin template (that is, **3**), forming **6** in a 43% yield. The ^{1}H NMR spectrum of **6** showed no signals originating from the porphyrin core, and the UV–vis. spectrum of **6** showed no detectable absorbance at 420 nm, the Soret band of the porphyrin. Elemental analysis of the hydrolysis product was consistent with a

dodecahydrate of **6** containing 30 cross-links. Elemental analysis for both nitrogen and ruthenium showed none present (0.0 ± 0.3%) and only a trace of potassium. Finally, comparison of the MALDI–TOF mass spectra of **5** and **6** showed the peaks in the latter shifted to lower *m/z* values by 597 (see Supplementary Information), corresponding to the loss of the porphyrin core ($C_{44}H_{14}N_4$: *m/z* 598.6).

The hydrolysis reaction that removes the template molecule H_2T(3,5-OHPh)P (**3**) results in the addition of eight –OH groups inside the dendrimer host, so **3** does not generate an ideal imprint for binding of itself (Fig. 2). In the limit of a well-formed imprint, the hydrolysis reaction creates a binding site that is too small to accommodate **3**, but might be suitable for the isomeric hydroxy compound, H_2T(2,6-OHPh)P (**7**) or tetrapyrimidyl porphyrin (H_2T(3,5-pyrimidyl)P) **8**. An extensive series of porphyrins, **7**–**16** (Fig. 3), was therefore prepared[26,27], and used to study the binding of imprinted dendrimer **6**.

To conduct the binding experiments, the solvent had to be sufficiently apolar to allow formation of hydrogen bonds, but polar enough to dissolve both **6** and the porphyrin. The complexation studies with octahydroxyporphyrins **3** and **7** were performed in 5% (v/v) ethyl acetate–toluene, whereas **8**–**16** were sufficiently soluble to study in toluene. Spectrophotometric titrations were performed by adding aliquots of a concentrated solution of imprinted dendrimer to a dilute solution of porphyrin and recording the Soret region after 10 minutes of equilibration.

Complexation of porphyrin **7** by imprinted dendrimer **6** was signalled by a significant bathochromic (red) shift in the λ_{max} of the Soret band of **7** (3 μM solution in 5% ethyl acetate–toluene) upon addition of **6** (see Supplementary Information). Consistent with hydrogen-bond complexation, the red shift could be fully reversed by increasing the ethyl acetate content from 5% (v/v) to >15% (v/v) in toluene. Furthermore, no red shift was observed when **6** was added to a solution of **7** in 50% (v/v) ethyl acetate–toluene. In 5% ethyl acetate–toluene no change in the Soret band of H_2TPP (**9**) or H_2T(3,5-OHPh)P (**3**) occurred upon addition of **6**. The latter result argues for a relatively rigid imprint; that is, **6** is not a flexible octa-acid that can complex any guest with sufficient hydrogen bond donors or acceptors. The magnitude of the shift in the Soret band of **7** was directly dependent on the amount of **6** added and the time elapsed. Extensive studies to be published separately indicate a relatively homogeneous imprint that produces within two hours a complex with a 5 nm red shift and a diminished apparent extinction coefficient, which, in turn, undergoes a slow conformation change over 17 days producing a tighter complex (10-fold increase in apparent association constant K_{app}) with an additional 6 nm red shift and an increased apparent extinction coefficient. The results described below are for the fast binding process only.

Complexation of H_2T(2,6-OHPh)P (**7**) by imprinted dendrimer **6** was also observed by SEC. Porphyrin **7** does not elute from the SEC matrix by itself, but in the presence of the imprinted dendrimer **6** it elutes with a measured retention time identical to that of the dendrimer. Thus, complexation within the dendrimer protects the polar porphyrin from adsorption during the course of its elution and decomplexation is slow on the timescale of the SEC experiment (minutes).

To determine the shape selectivity and number of binding contacts to the ligand, quantitative binding studies were carried out with porphyrins **7**–**16** (Fig. 3) using standard methods[28]. The

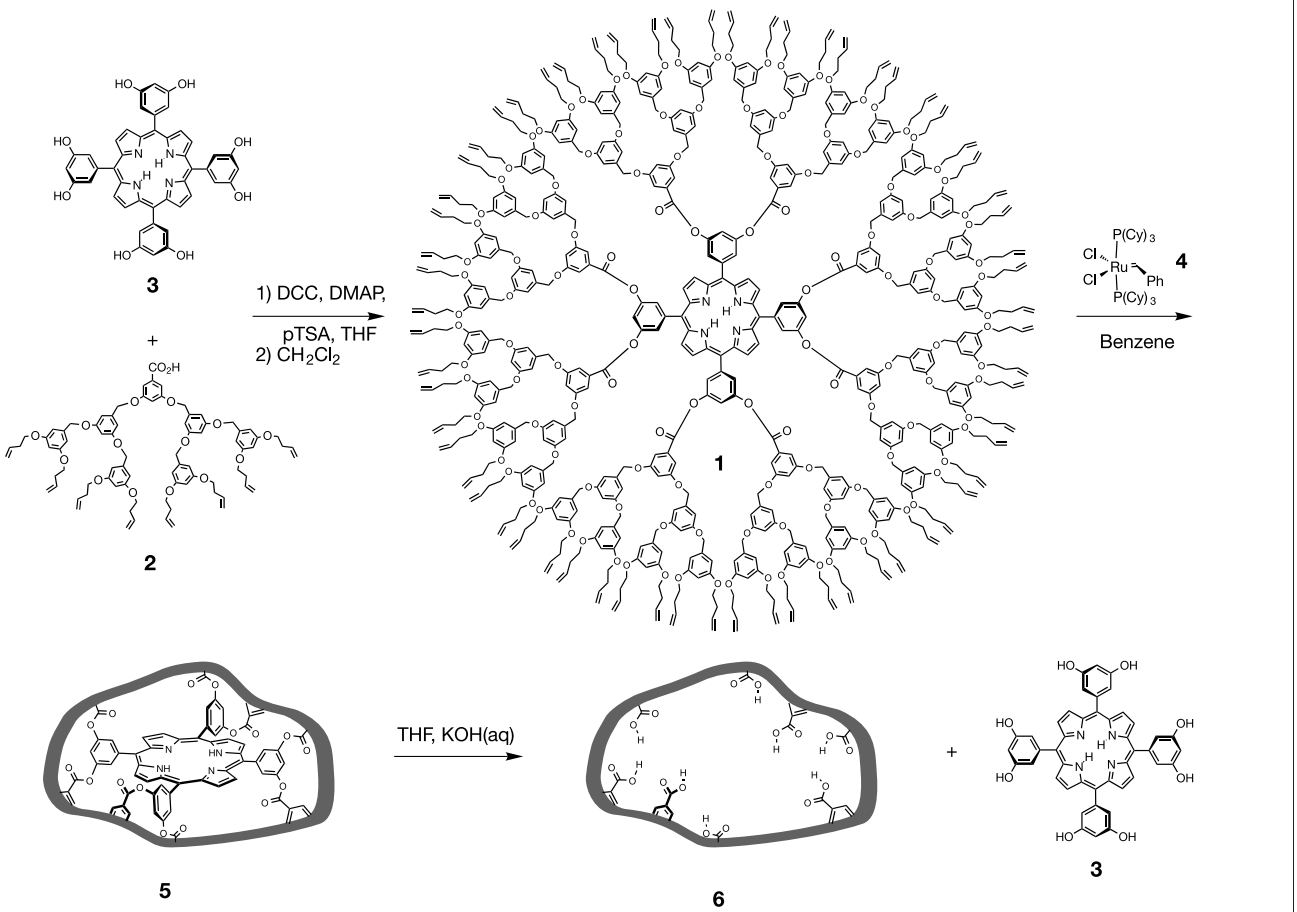

Figure 1 Scheme illustrating the preparation of imprinted dendrimer **6**. First, dendrons **2** are attached to the core porphyrin **3** to produce the dendrimer **1**, then **1** is cross-linked using Grubbs' catalyst **4** to give the dendrimer **5**, followed by the hydrolysis of **5** to remove the porphyrin core **3** and produce **6**. DCC, dicyclohexylcarbodiimide; DMAP, 4-(dimethylamino)pyridine; pTSA, *p*-toluene sulphonic acid; THF, tetrahydrofuran.

association constants (Fig. 3) are denoted as K_{app} because of the likely heterogeneity in **6** and time dependence of the binding process. H_2T(3,5-pyrimidyl)P (**8**) is bound by **6** with a K_{app} ($5 \times 10^4\,M^{-1}$) of the same magnitude as the **6**·**7** association. The pyridyl porphyrins H_2T(2-pyridyl)P (**10**), H_2T(3-pyridyl)P (**11**) and H_2T(4-pyridyl)P (**12**) bind equally well, despite their capacity to make only half as many hydrogen bonds as **8**. Although this may suggest that the full eight carboxylic acids are not simultaneously engaged in binding H_2T(3,5-pyrimidyl)P (**8**), the difference must partly originate in the 10^4-fold higher basicity of pyridine relative to pyrimidine. Along the same lines, given that typical pyridine–carboxylic acid association constants in apolar organic solvents are $\sim 10^2\,M^{-1}$, it might be expected that complexes containing at least four such interactions would exhibit absolute K_{app} values higher than 10^4 to $10^5\,M^{-1}$. Factors that may lower the K_{app} values for **6** include the need to break any internal carboxylic acid dimers or otherwise conformationally reorganize the binding site, and remove water molecules bound to the carboxylic acid groups. Although infrared studies of **6** were inconclusive with respect to possible dimerization of its carboxylic groups, elemental analysis of **6** indicates the presence of water presumably solvating the polar core. The K_{app} for the **6**·**10** (2-pyridyl isomer) is approximately 2-fold lower than that for the 3- and 4-pyridyl isomers **11** and **12**, indicating a degree of shape selectivity in the imprint. No binding was detected for tetraphenyl, mono, bis, and trispyridyl porphyrins **9**, **13**, **14**, **15** or **16**. Thus, a minimum of four binding contacts is necessary for complexation under the conditions used in this study.

To further support the importance of reversible complexation by hydrogen bonding and the direct involvement of the carboxylic acid groups, the octa-ethyl ester dendrimer **6**-$(CO_2Et)_8$ was prepared by ethanolysis of **5** (K_2CO_3, toluene, ethanol, reflux). The structure of **6**-$(CO_2Et)_8$ was verified by SEC, ^{1}H NMR spectroscopy, MALDI–TOF mass spectrometry, and UV–vis. spectroscopy. The addition of approximately 60 equivalents of **6**-$(CO_2Et)_8$ to H_2T(3-pyridyl)P (**11**) caused no red shift over the course of 4 days. Likewise addition of simple carboxylic acids did not cause a red shift of H_2T(3-pyridyl)P (**11**). Neither the addition of 640 equivalents of dendron carboxylic acid **2** to a $\sim 3\,\mu M$ solution of H_2T(2,6-OHPh)P (**7**) in 5% ethyl acetate–toluene nor the addition of 2,000 equivalents of 4-*t*-butyl benzoic acid to a $\sim 3\,\mu M$ solution of H_2T(3-pyridyl)P (**11**) in toluene led to any red shift. Finally, a smaller dendrimer with three acid groups, which was imprinted with 1,3,5-tri(hydroxymethyl)benzene[12], did not alter the position of the Soret band of a $\sim 3\,\mu M$ solution of **11** in toluene even upon addition of 49 equivalents.

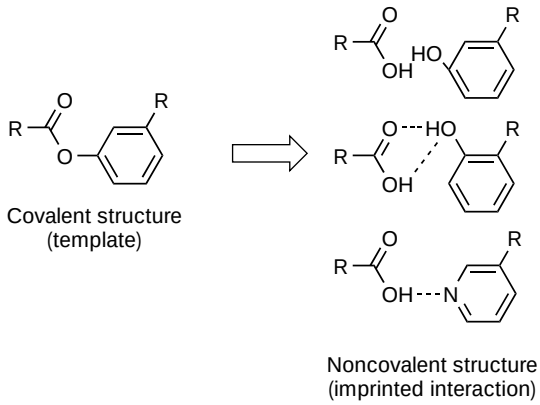

Figure 2 Structural drawing illustrating structural changes that occur upon hydrolysis of the cross-linked dendrimer **5**. The covalent structure contains eight phenyl benzoates formed by esterification of the phenolic porphyrin **3** with the carboxylic acid dendrons **2**. Note that two oxygen atoms would be left in the same space if both components of the covalent structure were held fixed. The isomeric phenol is better accommodated and phenyl benzoate appears to imprint well for a 3-pyridyl or 3,5 pyrimidyl porphyrin.

As indicated above, a known source of heterogeneity in the imprinted dendrimer arises from incomplete reaction of **2** with **3**. This imperfect material was shown not to play a role in binding by carefully removing it with repeated preparative SEC. A different type of heterogeneity may originate in the RCM reaction of dendrimer **1**, which can produce **5** containing a very large number of cross-link isomers. The broad peaks observed in the ^{1}H NMR of **5** and **6** might be attributed to the presence of a mixture of such isomers, although the heterogeneity does not manifest itself in the binding (see above).

To gain insight into the three-dimensional structure of **6** and how it changes with the extent and position of the cross-links, molecular modelling was performed using molecular mechanics and dynamics. A series of cross-linked dendrimers **5** were built and minimized. The porphyrin core was removed, providing a globular porous structure with eight carboxyl groups in its interior. The resulting models of **6** were subjected to 60 ps of molecular dynamics alone and with H_2T(3,5-pyrimidyl)P (**8**) within the binding site. In both cases the overall globular shape of **6** did not significantly change compared to that of **5**. The van der Waals surface of a modelled imprinted dendrimer with nine intra- and 20 inter-dendron cross-links (Fig. 4a) reveals a slightly porous structure with no obvious large channels to the binding site. Thus, complexation and decomplexation must involve a dynamic breathing process (in other models with a higher fraction of intra-dendron cross-

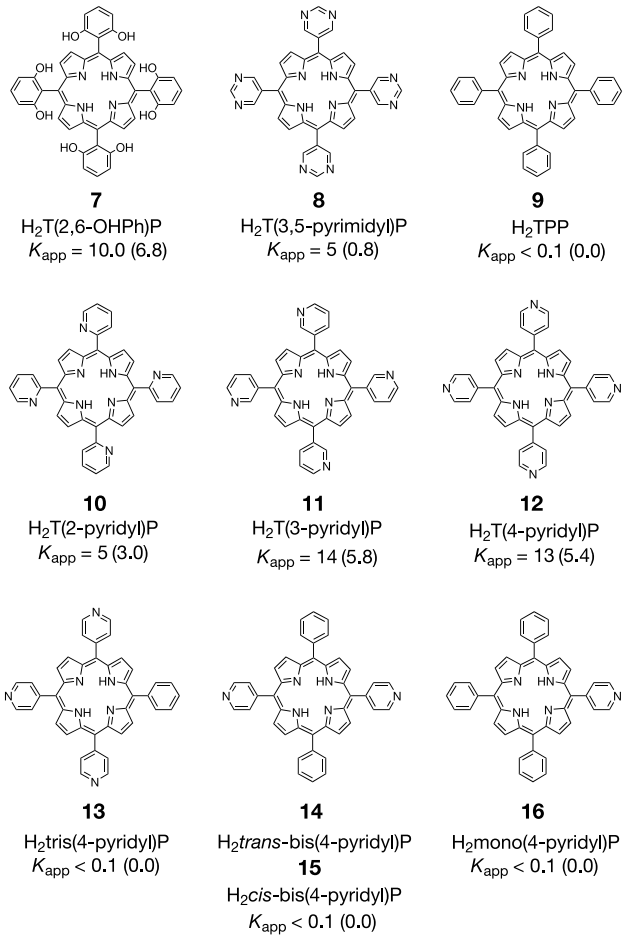

Figure 3 Porphyrins used to study binding properties of imprinted dendrimer **6**. Each structure is accompanied by the corresponding apparent association constant K_{app} ($\times 10^4\,M^{-1}$), and the red shift value of the Soret band ($\Delta\lambda_{max}$, nm) for the complex formed between imprinted dendrimer **6** and the porphyrin. A value of $\Delta\lambda_{max} = 0.0$ indicates no observed change in the absorption spectrum. Upper limits on solubility prevented a more accurate upper limit of K_{app} from being obtained.

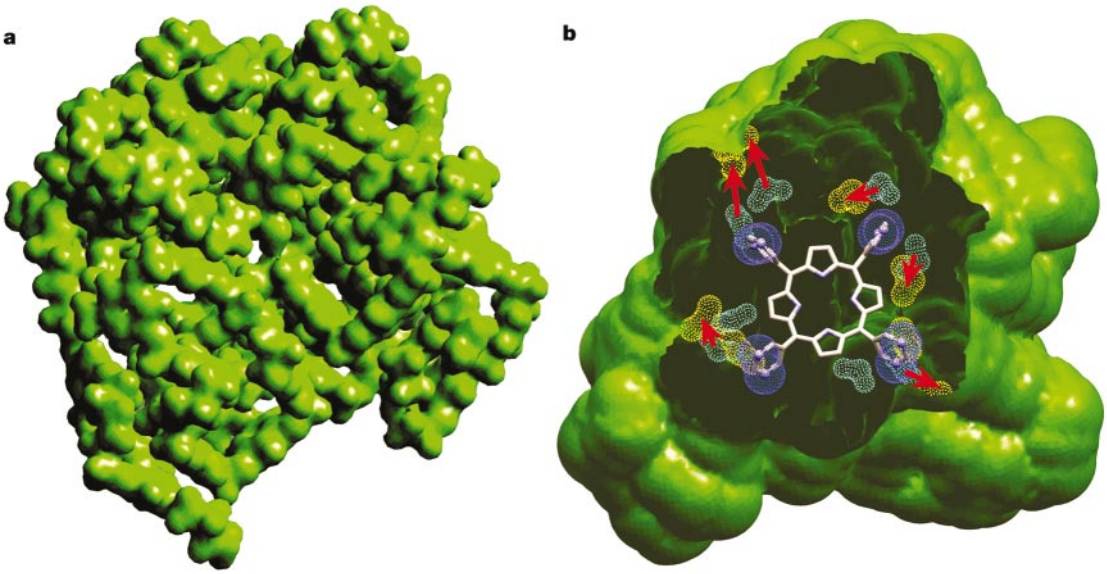

Figure 4 Calculated structure of imprinted dendrimer **6** built by iterative attachment of dendrons to the core porphyrin, minimization and cross-linking of neighbouring double bonds. **a**, van der Waals surface of a representative dendrimer structure produced by a 60 ps annealed dynamics simulation. **b**, Calculated binding pocket inside **6**; yellow clouds represent positions of carboxyl groups when **6** is minimized without the host porphyrin **8**, cyan clouds represent positions of carboxyl groups when **6** is minimized in the presence of the host porphyrin **8**, red arrows show the movement of carboxylic groups.

links, the binding pocket appears more readily accessible). The carboxyl groups in **6** moved from their original positions in the ester links of **5**, but the binding pocket was mostly intact (Fig. 4b). The displacement of carboxyl groups was less significant when **8** was present in the interior of the cored dendrimer as seen in the overlaid structures in Fig. 4b.

As a demanding test of the monomolecular imprinting process, we chose a particularly large molecule guest, a polyfunctionalized porphyrin, as the template within an octa-dendron array. Extensive cross-linking using the RCM reaction followed by template removal produced an imprinted dendrimer that selectively and tightly ($K_{app} = (0.5–1.4) \times 10^5\,M^{-1}$) bound porphyrins presenting an appropriate size and four or more hydrogen-bonding sites (for example, **7**, **8**, **10**–**12**). The binding is size selective on the basis of results with the octahydroxyl porphyrins **3** and **7**, and modestly shape-selective on the basis of the results with the isomeric pyridyl porphyrins (**10**–**12**).

The limitations of this approach are the need for multi-step synthesis of the dendrimers, and the high dilution conditions needed for the RCM reaction. (We note that it was recently shown that this high dilution is not necessary for a dendrimer where the alkene groups reside in the branching units[13].) But even in its current implementation, the monomolecular imprinting approach has several characteristics not yet obtainable through traditional polymer imprinting. These include high-efficiency imprinting with nearly all templates producing functional binding sites, quantitative removal of the template, solubility of the imprinted material in common organic solvents, and separation of imperfectly assembled binding sites. By using resins covalently linked to the target ligand, it should be possible to fractionate heterogeneous material after imprinting. In this manner, selection of imprinted sites on the basis of affinity or binding kinetics should be possible. Finally, the single-step synthesis of hyperbranched or analogous macromolecules, combined with the ability to integrate reporter groups, makes the monomolecular imprinting approach a promising one for further development. □

Methods

The titration data were analysed by plotting [ID] against [ID]/ΔA, where [ID] is the imprinted dendrimer concentration and ΔA is the change in absorbance upon addition of **6**. This method allows association constants to be determined by finding the line intercept that gives $1/K_{app}$, and does not require knowledge of the concentration of the free or complexed porphyrin. The titrations were all completed within 1 h and all gave linear plots. As with other Scatchard-type plots, linearity indicates the formation of 1:1 complexes.

Molecular mechanics and dynamics were performed using Cerius[2], version 4.5 (Accelrys). For energy minimizations and simulated annealing (60 ps, 300–500 K), the Dreiding force field was used.

Preparation of 1

Compound **1** (5,10,15,20-tetrakis{3,5-bis[3,5-bis(3,5-bis(3,5-bis(3-buten-1-oxy)benzyloxy)benzyloxy)benzoyloxy]phenyl}porphyrin ([G-3]$_8$-T(3,5-OHPh)P)) was synthesized as follows. [G-3]-CO_2H (**2**) (283 mg, 215 μmol), 13.2 mg (17.8 μmol) of **3** (5,10,15,20-tetrakis(3′,5′-dihydroxyphenyl)porphyrin, referred to as H_2T(3,5-OHPh)P), 519 mg (2.5 mmol) of dicyclohexylcarbodiimide (DCC), 78.6 mg (643 μmol) of 4-(dimethylamino)pyridine (DMAP) and 118 mg (621 μmol) of *p*-toluene sulphonic acid (pTSA) were dissolved in 15 ml of THF. The reaction mixture was stirred overnight at room temperature and filtered to remove the dicyclohexylurea (DCU) formed. The filtrate was concentrated under reduced pressure and dissolved in 15 ml of CH_2Cl_2. To this solution, 510 mg (2.5 mmol) of DCC, 75.8 mg (620 μmol) of DMAP and 117 mg (615 μmol) of pTSA was added, and the mixture was stirred at room temperature. The reaction was complete after three days (by thin-layer chromatography and SEC). The reaction mixture was filtered to remove the DCU, and the resulting filtrate was concentrated under reduced pressure. The remaining residue was loaded onto a silica gel column (4 × 15 cm) and eluted with 30% EtOAc/PE. The product was further purified by loading it onto a SEC column and eluting it with toluene. The product was dried overnight under vacuum to afford 107 mg (54%) of **1** as a deep red oil: ^{1}H NMR (CD_2Cl_2) δ 9.22 (s, 8H), 8.15 (d, 8H), 7.75 (t, 4H), 7.54 (d, 16H), 6.81 (t, 8H), 6.64 (d, 32H), 6.48 (m, 80H), 6.31 (t, 32H), 5.81 (ddt, 64H), 5.07 (ddt, 64H), 5.01 (ddt, 64H), 4.98 (s, 32H), 4.87 (s, 64H), 3.88 (t, 128H), 2.42 (tddd, 128H), −2.86 (s, 2H); ^{13}C NMR (CD_2Cl_2) 165.1, 160.7, 160.5, 160.4, 150.3, 144.2, 139.6, 139.3, 135.0, 131.6, 126.3, 118.9, 117.0, 109.3, 108.1, 106.7, 106.2, 101.9, 101.0, 70.5, 70.3, 67.6, 33.9; MS (MALDI–TOF) *m/z* 11,174.7 ($M + Na^+$); SEC (toluene) calculated $M_w = 8{,}155$; UV–vis. (CH_2Cl_2) $\lambda_{max} = 275.0$, 420.5 (Soret). Analysis: calculated for $C_{692}H_{734}N_4O_{128}$: C, 74.51; H, 6.63; N, 0.50. Found: C, 74.56; H, 6.41; N, 0.48.

Cross-linked [G-3]$_8$-T(3,5-OHPh)P (5)

To a solution of 497 mg (44.6 μmol) of **1** in 4.4 litres of benzene was added 99.6 mg (120 μmol) of Grubbs' catalyst (**4**). The reaction mixture was stirred at room temperature for 22 h. The benzene was removed under reduced pressure. The crude product was loaded onto a silica gel plug (4 × 6 cm) and eluted with 400 ml of 50% petroleum ether/50% CH_2Cl_2 and 400 ml of 5% EtOAc/CH_2Cl_2. The EtOAc/CH_2Cl_2 solution was concentrated under reduced pressure. The product was dried overnight under vacuum to afford 409 mg (89%) of **5** as a dark red powder: ^{1}H NMR (d_8-toluene) δ 9.17 (bs, 8H), 8.15 (bs, 8H), 7.70 (bs, 20H), 6.59 (bs, 152H), 5.78 (bs, ~4H), 5.51 (bs, ~60H), 5.04 (bs, ~8H), 4.82 (bs, 96H), 3.70 (bs, 128H), 2.33 (bs, 128H); MS (MALDI–TOF) *m/z* 10,258.2 ($M + H^+ - 32C_2H_4$), 10,286.3 ($M + H^+ - 31C_2H_4$), 10,311.8 ($M + H^+ - 30C_2H_4$); SEC (toluene) calculated $M_w = 5509$; UV–vis. (CH_2Cl_2) $\lambda_{max} = 276.0$, 421.0 (Soret).

Imprinted [G-3]$_8$-T(3,5-OHPh)P (6)

To a solution of 102 mg (9.88 μmol) of **5** dissolved in 15 ml of THF, was added 10 ml of 2.5 M aqueous KOH. The reaction mixture was stirred vigorously at reflux until the reaction was complete by TLC. The reaction was stopped by removing the THF under reduced pressure. The resulting aqueous layer was extracted with $CHCl_3$ (3 × 25 ml). The combined organic layers were washed with 1 M aqueous HCl and water, and concentrated under reduced pressure. The product was dried under vacuum to afford 41.5 mg (43%) of **6** as a beige powder: ^{1}H NMR δ 7.23 (bs, 16H), 6.51 (bs, 152H), 5.86 (bs, ~4H), 5.60 (bs, ~60H), 5.12 (bs, ~8H), 4.86 (bs, 96H), 3.92 (bs, 128H), 2.45 (bs, 128H); MS (MALDI–TOF) *m/z* 9,710.8 ($M + Na^+ - 31C_2H_4 - C_{44}H_{14}N_4$), 9,756.0 ($M + K^+ - 30C_2H_4 - C_{44}H_{14}N_4$), 9,779.8 ($M + K^+ - 29C_2H_4 - C_{44}H_{14}N_4$), 9,810.7 ($M + K^+ - 28C_2H_4 - C_{44}H_{14}N_4$). Analysis: calculated for $C_{588}H_{600}O_{128}$: C, 72.70; H, 6.22; N, 0.00; Ru, 0.00. Found: C, 70.83; H, 6.19; N, 0.00; Ru, 0.00.

Received 28 February; accepted 28 May 2002; doi:10.1038/nature00877.

1. Wulff, G. & Sarhan, A. The use of polymers with enzyme-analogous structures for the resolution of racemates. *Angew. Chem. Int. Edn Engl.* **11,** 341–343 (1972).
2. Shea, K. J. Molecular imprinting of synthetic network polymers: the de novo synthesis of macromolecular binding and catalytic sites. *Trends Polym. Sci.* **2,** 166–173 (1994).
3. Andersson, L., Sellergren, B. & Mosbach, K. Imprinting of amino acid derivatives in macroporous polymers. *Tetrahedr. Lett.* **25,** 5211–5214 (1984).
4. Katz, A. & Davis, M. E. Molecular imprinting of bulk, microporous silica. *Nature* **403,** 286–289 (2000).
5. Wulff, G. Molecular imprinting in cross-linked materials with the aid of molecular templates—a way towards artificial antibodies. *Angew. Chem. Int. Edn Engl.* **34,** 1812–1832 (1995).
6. Katz, A. & Davis, M. Investigations into the mechanisms of molecular recognition with imprinted polymers. *Macromolecules* **32,** 4113–4121 (1999).
7. Sellergren, B. & Shea, K. J. Influence of polymer morphology on the ability of imprinted network polymers to resolve enantiomers. *J. Chromatogr.* **635,** 39–41 (1993).
8. Vlatakis, G., Andersson, L. I., Muller, R. & Mosbach, K. Drug assay using antibody mimics made by molecular imprinting. *Nature* **361,** 645–647 (1993).
9. Lehn, J.-M. & Eliseev, A. V. Dynamic combinatorial chemistry. *Science* **291,** 2331–2332 (2001).
10. Cousins, G. R. L., Poulsen, S.-A. & Sanders, J. K. M. Molecular evolution: dynamic combinatorial libraries, autocatalytic networks and the quest for molecular function. *Curr. Opin. Chem. Biol.* **4,** 270–279 (2000).
11. Klekota, B. & Miller, B. L. Dynamic diversity and small-molecule evolution: a new paradigm for ligand identification. *Trends Biotechnol.* **17,** 205–209 (1999).
12. Wendland, M. S. & Zimmerman, S. C. Synthesis of cored dendrimers. *J. Am. Chem. Soc.* **121,** 1389–1390 (1999).
13. Schultz, L. G., Zhao, Y. & Zimmerman, S. C. Synthesis of cored dendrimers with internal cross-links. *Angew. Chem. Int. Edn Engl.* **40,** 1962–1966 (2001).
14. Newkome, G. R., Moorefield, C. N. & Vögtle, F. *Dendrimers and Dendrons: Concepts, Syntheses, Perspectives* (Wiley-VCH, Weinheim, 2001).
15. Sanders, J. K. M. Templated chemistry of porphyrin oligomers. *Compreh. Supramolec. Chem.* **9,** 131–164 (1996).
16. Rakow, N. A. & Suslick, K. S. A colorimetric sensor array for odour visualization. *Nature* **406,** 710–714 (2000).
17. Matsui, J., Higashi, M. & Takeuchi, T. Molecularly imprinted polymer as 9-ethyladenine receptor having a porphyrin-based recognition center. *J. Am. Chem. Soc.* **122,** 5218–5219 (2000).
18. Ogoshi, H. & Mizutani, T. Novel approaches to molecular recognition using porphyrins. *Curr. Opin. Chem. Biol.* **3,** 736–739 (1999).
19. Bhyrappa, P., Young, J. K., Moore, J. S. & Suslick, K. S. Dendrimer-metalloporphyrins: synthesis and catalysis. *J. Am. Chem. Soc.* **118,** 5708–5711 (1996).
20. Dandliker, P. J., Diederich, F., Gisselbrecht, J.-P., Louati, A. & Gross, M. Water-soluble dendritic iron porphyrins: synthetic models of globular heme proteins. *Angew. Chem. Int. Edn Engl.* **34,** 2725–2728 (1996).
21. Sadamoto, R., Tomioka, N. & Aida, T. Photoinduced electron transfer reactions through dendrimer architecture. *J. Am. Chem. Soc.* **118,** 3978–3979 (1996).
22. Balzani, V. *et al.* Dendrimers based on photoactive metal complexes. Recent advances. *Coord. Chem. Rev.* **219–221,** 545–572 (2001).
23. Hawker, C. J. & Frechet, J. M. J. A new convergent approach to monodisperse dendritic macromolecules. *J. Am. Chem. Soc.* **112,** 7638–7647 (1990).
24. Trnka, T. M. & Grubbs, R. H. The development of L_2X_2Ru = CHR olefin metathesis catalysts: an organometallic success story. *Acc. Chem. Res.* **34,** 18–29 (2001).
25. Coates, G. W. & Grubbs, R. H. Quantitative ring-closing metathesis of polyolefins. *J. Am. Chem. Soc.* **118,** 229–230 (1996).
26. Adler, A. D. *et al.* A simplified synthesis of *meso*-tetraphenylporphyrin. *J. Org. Chem.* **32,** 476 (1967).
27. Rho, T. & Abuh, F. One-pot synthesis of pyrimidine-5-carboxaldehyde and ethyl pyrimidine-5-carboxylate by utilizing pyrimidin-5-yl-lithium. *Synth. Commun.* **24,** 253–256 (1994).
28. Collman, J. P. *et al.* Oxygen binding to cobalt porphyrins. *J. Am. Chem. Soc.* **100,** 2761–2766 (1978).

Supplementary Information accompanies the paper on *Nature*'s website (http://www.nature.com/nature).

Acknowledgements

We thank W.A. Goddard and T. Cagin for help with dendrimer modelling. This work was funded by the NIH and the US Army Research Office. I.Z. thanks the Arnold and Mabel Beckman Foundation for a Beckman fellowship.

Competing interests statement

The authors declare that they have no competing financial interests.

Correspondence and requests for materials should be addressed to S.C.Z. (e-mail: sczimmer@uiuc.edu).

Tungsten isotope evidence from ~3.8-Gyr metamorphosed sediments for early meteorite bombardment of the Earth

Ronny Schoenberg*, Balz S. Kamber*, Kenneth D. Collerson* & Stephen Moorbath†

** Advanced Centre for Queensland University Research Excellence (ACQUIRE), The University of Queensland, St Lucia, Queensland 4072, Australia*
† Department of Earth Sciences, University of Oxford, Parks Road, Oxford OX1 3PR, UK

The 'Late Heavy Bombardment' was a phase in the impact history of the Moon that occurred 3.8–4.0 Gyr ago, when the lunar basins with known dates were formed[1,2]. But no record of this event has yet been reported from the few surviving rocks of this age on the Earth. Here we report tungsten isotope anomalies, based on the ^{182}Hf–^{182}W system (half-life of 9 Myr), in metamorphosed sedimentary rocks from the 3.7–3.8-Gyr-old Isua greenstone belt of West Greenland and closely related rocks from northern Labrador, Canada. As it is difficult to conceive of a mechanism by which tungsten isotope heterogeneities could have been preserved in the Earth's dynamic crust–mantle environment from a time when short-lived ^{182}Hf was still present, we conclude that the metamorphosed sediments contain a component derived from meteorites.

It is widely conjectured that the Earth suffered contemporaneous Late Heavy Bombardment (LHB) with the Moon, scaled up proportionally to its much greater gravitational cross-section. Earth's estimated[3] mass accretion rate during the LHB was of the order of $(1–2) \times 10^{15}$ g yr^{-1}, or $(2–4) \times 10^{-4}$ g cm^{-2}. Over a 100-Myr period of LHB, this accretion rate would have yielded $(1–2) \times 10^{23}$ g of material. If added as a continuous veneer over the entire planet, this would correspond to 200 t m^{-2}. The distinct deuterium/hydrogen ratio of the terrestrial hydrosphere[4] argues against significant cometary accretion, whereas compositions of projectiles in lunar impact melts[5] indicate infall from asteroids of enstatite chondrite or iron meteorite parentage. Thus, unless the Earth's early crust was continually recycled into the mantle, it should be possible to detect chemical 'fingerprints' of the LHB in the oldest terrestrial sediments.

In a recent study[6], the extinct radioactive decay scheme ^{53}Mn–^{53}Cr (half-life, 3.7 Myr) was used to detect meteoritic infall in Cretaceous/Tertiary (K/T) boundary sediments. As Cr isotopes in all classes of meteorites and terrestrial samples are distinct, discovery of a non-terrestrial Cr isotope composition[6] confirmed extraterrestrial origin. A similar opportunity for detecting meteoritic infall is afforded by the ^{182}Hf–^{182}W system (half-life, 9 Myr). By analogy with the homogeneous terrestrial Cr isotope composition[6], any variations in W isotope composition that may have existed in the first ~60 Myr of Earth's history would have been homogenized by convection in the early mantle. Therefore the terrestrial W isotope composition is constant[7,8]. Indeed, all our terrestrial samples other than the early Archaean metamorphosed sediments (metasediments) yield a constant ^{182}W/^{183}W ratio (Fig. 1 and Table 1) of 0.10 ± 0.22 ε_W units (where ε_W is the deviation, in 0.1‰, from the terrestrial ^{182}W/^{183}W ratio), identical to our standard (ACQUIRE-W), which was reproduced at 0.00 ± 0.10 ε_W.

In contrast, a well-resolved W isotope variability exists among different classes of meteorites. Iron meteorites[9] have much lower ^{182}W/^{183}W ratios (Fig. 1) of, on average, −3.7 ε_W, reflecting removal of metal-loving W from silicate into the core of planete-